CHEMICAL ENGINEERING TRANSACTIONS
VOL. 73, 2019
A publication of AIDIC
The Italian Association of Chemical Engineering
Online at www.aidic.it/cet
Guest Editors: Andrea D'Anna, Paolo Ciambelli, Carmelo Sunseri

ISBN 978-88-95608-70-9; **ISSN** 2283-9216
DOI: 10.3303/CET1973023

H_2 Generation via Ethanol Reforming over CeO_2-SiO_2 Based Catalysts

Vincenzo Palma, Concetta Ruocco*, Antonio Ricca

Department of Industrial Engineering, University of Salerno, Via Giovanni Paolo II 132, 84084, Fisciano (SA) Italy
cruocco@unisa.it

In this paper, the renewable hydrogen generation through oxidative steam reforming of ethanol has been investigated over bimetallic Pt-Ni/CeO_2-SiO_2 catalysts, prepared by sequential wet impregnation at different loadings of noble metals (0-3 wt%); temperature ranged from 300 to 600°C and the H_2O/C_2H_5OH as well as O_2/C_2H_5OH ratios were fixed, respectively, to 4 and 0.5. The samples were characterized by BET, XRD and TPR analysis. Despite the very low contact time selected (25 ms), all the bimetallic samples displayed ethanol conversions higher than 50% above 450°C; however, the selectivity in hydrogen generation decreased with the Pt content. It indicates that low platinum loading are sufficient to assure a promising performance for the investigated reaction, thus assuring a considerable reduction of the catalyst cost. An experimental kinetic investigation was also carried out on the most interesting bimetallic sample in comparison with the monometallic catalyst in order to predict the evolution of product species with reaction temperature.

1. Introduction

The research activities focused on the production of energy carriers from bio-resources are attracting increasing interest, due to the gradual depletion of fossil fuel reserves and the efforts to control environmental pollution (Hernández et al., 2018). For example, bioethanol produced from biomass is considered to be a promising source both for the production of transportation fuels and to fulfil the increasing demand of hydrogen for use in fuel cells. Bioethanol is more attractive compared to methane because of its easy storage, low toxicity and its potential to be produced in a more economic and competitive manner from non-edible lignocellulose. Bioethanol conversion via steam reforming is an attractive route for the valorisation of this biofuel. In fact, the energy demanding water separation units necessary for upgrading bioethanol as fuel can be avoided and the theoretically produced hydrogen per mole of reacted ethanol is very high compared to other conversion processes (Mulewa et al., 2017). Despite the choice of steam to ethanol ratios higher than the stoichiometric values can mitigate catalyst deactivation by coke deposition and assure improved hydrogen selectivties, the occurrence of unwanted pathways may negatively affect H_2 production rate due to the formation of secondary products (including acetone, acetaldehyde and ethylene) (Montero et al., 2014). Thus, the development of ethanol steam reforming at an industrial scale requires the formulation highly active and selective catalysts. On the other hand, ethanol steam reforming is highly endothermic and the addition of energy supply is needed which, together with the necessary high operation temperatures, leads to a considerable increase of both fixed and operative costs. At that end, oxidative steam reforming of ethanol provides a viable route to eliminate external heat requirements. Moreover, the addition of O_2 to the ethanol/water vapours reduces the risk of carbon formation on catalyst surface, promoting, at the same time, the oxidation of coke already deposited (Morales and Segarra, 2015). Oxidative steam reforming of ethanol has been investigated over numerous monometallic and bimetallic formulations (Baruah et al., 2015). The employment of catalyst containing more than one active species, in fact, was shown to improve catalyst activity and stability for ethanol reforming (Palma et al., 2015).
In our previous work, we demonstrated that a bimetallic 3wt% Pt-10wt% Ni catalyst supported on CeO_2-SiO_2 is able to assure carbon formation rates among the lowest found in the recent literature (Palma et al., 2017). However, the platinum content in the catalyst can strongly affect its final cost. Thus, in the attempt to develop less expensive formulations, in the present work, Pt content was varied in the interval 0-3 wt% and its effect

Paper Received: 09 July 2018; Revised: 03 October 2018; Accepted: 10 January 2019

Please cite this article as: Palma V., Ruocco C., Ricca A., 2019, H2 Generation via Ethanol Reforming over Ceo2-sio2 Based Catalysts , Chemical Engineering Transactions, 73, 133-138 DOI:10.3303/CET1973023

on catalyst activity for oxidative steam reforming of ethanol (OESR) was investigated. A kinetic analysis was also carried out on the most promising sample, studied in comparison with the monometallic Ni-based catalyst.

2. Experimental

2.1 Catalyst preparation and characterization

The CeO_2-SiO_2 mixed oxide was prepared by impregnation of calcined mesoporous silica gel (SigmaAldrich, 90-115 μm) with a cerium nitrate (Strem Chemicals) solution at 80°C for 2 hours. After filtration, the solid was dried at 120°C and calcined in air at 600°C for 3 hours. Platinum was deposited on the Ni/CeO_2-SiO_2 sample through a further impregnation-drying-calcination step starting from a solution of platinum chloride (Strem Chemicals). Four samples were prepared at platinum contents of 0.5, 1, 2 and 3 wt% and were denoted as 0.5Pt10Ni, 1Pt10Ni, 2Pt10Ni, 3Pt10Ni; the monometallic Ni/CeO_2-SiO_2 catalyst was indicated as 10Ni.
The specific surface area of the catalysts was determined by the BET method using a Sorptometer 1040 "Kelvin" from Costech Analytical Technologies; before the analysis, the samples were degassed at 150°C for 1 hour.
Powder X-ray diffraction (XRD) patterns were collected on a Brooker D8 using a scanning range of 20-80°.
H_2 temperature programmed reduction (TPR) was performed in situ in the laboratory apparatus described in Par. 2.2. The analysis was carried out by increasing the catalyst temperature from 25 to 700 °C 5 at 10 °C/min under a 5%H_2/N_2 flow. Starting from the area under the reduction peaks, it was possible to evaluate the experimental H_2 uptake; a comparison with the theoretical consumption (calculated on the basis of Ni as well as Pt loadings) was also provided.

2.2 Laboratory apparatus and procedure

Catalyst activity tests were conducted in a fixed-bed stainless steel reactor at atmospheric pressure. Typically, the catalyst (0.6 g, 180-355 μm) diluted with quartz (dilution ratio of 2, 500-710 μm) was loaded and sandwiched between two quartz flakes. After catalyst reduction in situ, the water/ethanol mixture (molar ratio of 4) was sent to a boiler for vaporization at a rate of 32 $g \cdot h^{-1}$; nitrogen (55 % by volume of the reacting mixture) was used as carrier gas and air was fed within the reactor (in correspondence of the catalytic bed) through an independent line. Activity measurements were performed between 300 and 600°C under a Weight Hourly Space Velocity (WHSV) of 62 h^{-1} (corresponding to a contact time of 25 ms); these very stressful conditions were selected to evaluate catalytic performances far from equilibrium. The reaction products were monitored online using an FT-IR Spectrophotometer (IGS Antaris from ThermoScientific); then, the mixture was passed through a cold trap and, after the separation of condensable species (water and un-reacted ethanol), was sent to an ABB block made up of a thermoconductivity and a paramagnetic analyser for the evaluation of hydrogen and oxygen contents, respectively. The performances of the investigated catalysts were evaluated through the conversion of ethanol (Eq.1), hydrogen yield (Eq. 2) and C-containing species yield (CO, CO_2, CH_4, Eq.3).

$$X_{C2H5OH} = \frac{mol_{C2H5OH,in} - mol_{C2H5OH,out}}{mol_{C2H5OH,in}} \cdot 100 \quad (1)$$

$$Y_{H2} = \frac{mol_{H2,out}}{6 \cdot mol_{C2H5OH,in}} \cdot 100 \quad (2)$$

$$Y_i = \frac{mol_{i,out}}{2 \cdot mol_{C2H5OH,in}} \cdot 100 \quad (3)$$

3. Results and discussion

3.1 Catalysts properties

Table 1 summarizes the results of catalyst characterization in terms of BET, XRD and TPR measurements.
The specific surface areas of the catalysts were denoted as S_{BET} while the average size of the crystallites with *d*. All the investigated catalysts displayed very high values of S_{BET} and only a slight decrease in the specific surface areas was observed as a result of the platinum content growth, ascribable to the PtO_X particles penetration in the mesopores of the support (Singh et al, 2017). XRD patterns of the CeO_2-SiO_2 based catalysts (Figure 1 (a)) mainly presented the four characteristic peaks located at 2Θ of 28.9°, 33.2°, 48.0° and

56.6° corresponding to (1 11),(2 00), (2 2 0), (311), respectively, which can be ascribed to the cubic structure of CeO_2 and sharp peaks at 2θ of 37.46° and 43.54°, relative to (1 1 1) and (2 0 0) crystal planes of NiO phase (Siang and Vo, 2017). However, no obvious signals of platinum phase were observed indicating highly dispersed and very small crystallites of PtO_x (the detection limit of XRD is normally above 3 nm (Zhao et al., 2018)). The average size of CeO_2 particles (7-8 nm) was unaffected by Pt loading growth while a slight effect was observed on NiO particles.

Table 1: Physiochemical properties and TPR results for the monometallic and bimetallic catalysts.

Sample	S_{BET} ($m^2 \cdot g^{-1}$)	d_{CeO2} (nm)	d_{NiO} (nm)	H_2 theoretical uptake ($\mu_{molH2} \cdot g_{cat}^{-1}$)	H_2 experimental uptake ($\mu_{molH2} \cdot g_{cat}^{-1}$)
10Ni	259	8	12	1704	2590
0.5Pt10Ni	256	7	10	1755	2953
1Pt10Ni	254	7	11	1806	3051
2Pt10Ni	242	7	12	1909	3245
3Pt10Ni	229	7	12	2011	3457

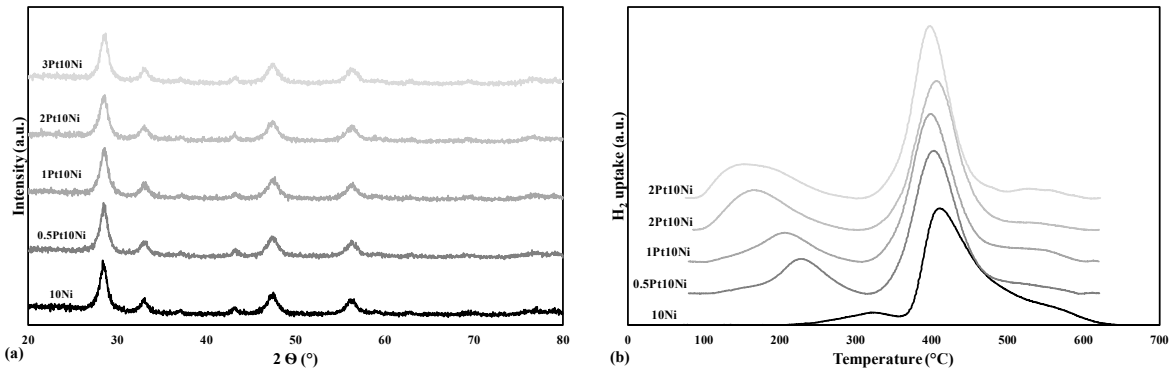

Figure 1: XRD patterns (a) and H_2-TPR profiles (b) of the CeO_2-SiO_2 supported catalysts.

TPR profiles of Pt-based bimetallic catalysts are shown in Figure 1 (b) in comparison with the reduction curve recorded over the Ni/CeO_2-SiO_2 sample. Two major reduction peaks are observed for every bimetallic catalyst, corresponding to the reduction of platinum and nickel oxides (Nishikawa et al., 2008). Two peaks with a shoulder at high temperatures were also observed for the monometallic Ni/CeO_2-SiO_2 sample, suggesting that three types of NiO species are present: aggregated NiO, highly dispersed NiO with strong interaction with the CeO_2 support and NiO incorporated into the ceria lattice (Du et al., 2012). The comparison between theoretical and experimental hydrogen consumption revealed that the interactions of NiO particles with the support promotes CeO_2 reduction. In fact, due to the occurrence of spillover phenomena (Takeguchi et al., 2001), H_2 uptake is higher than the expected value (2590 vs 1704 $\mu mol_{H2} \cdot g_{cat}^{-1}$). The effect of platinum deposition on the Ni/CeO_2-SiO_2 catalyst was the leftward shift of reduction peaks, which became more pronounced with the increase of noble metal loading, as well as a growth in the total hydrogen consumption. This result suggests that higher platinum contents reduce the Ni-CeO_2 degree of interaction, due to the formation of a Pt-Ni alloy (Palma et al., 2015): in fact, the reduction of the non-noble metal, driven by the diffusion of hydrogen molecules from the just reduced Pt particles towards the very close nickel phase, is progressively observed at lower temperatures. The growth in platinum content also assured higher catalyst reducibility, as attested by the H_2 uptake data reported in Table 1: in the case of 3Pt10Ni/CeO_2-SiO_2 catalyst, the H_2 consumption reached 3457 $\mu mol_{H2} \cdot g_{cat}^{-1}$, against a predicted value of 2011 $\mu mol_{H2} \cdot g_{cat}^{-1}$.

3.2 Activity of CeO_2-SiO_2 based catalysts and kinetic evaluations

The catalytic performances of Ni and PtNi catalysts for oxidative steam reforming of ethanol are preliminary compared in terms of ethanol conversion and hydrogen yield (Figure 2). Despite the reaction system operates far from equilibrium (Liu et al., 2008) for all the investigated catalysts, the trend of X_{C2H5OH} and Y_{H2} follows thermodynamic predictions: by increasing the reaction temperature, the endothermic steam reforming pathways are favoured, thus improving ethanol conversion and hydrogen production rates. In fact, at 600°C, all the samples assured total ethanol conversion and H_2 yield was close to 50%. The addition of Pt, whatever the selected content, positively affected catalyst performances, improving the behaviour of the monometallic

sample. However, it is worthwhile noting that the increase of noble metal content has a detrimental effect on both X_{C2H5OH} and Y_{H2}: the worst results, in fact, were recorded over the 3Pt10Ni/CeO_2-SiO_2 sample. On the other hand, the results displayed in Figure 2 demonstrate that very low Pt loadings are sufficient to allow the highest H_2 yields above 400°C. The activity results obtained over the 0.5Pt10Ni catalysts, in fact, were the most interesting and this formulation was selected to carry out a kinetic investigation; the 10Ni sample was also employed in this study for comparison.

The kinetic model developed to simulate and analyse the experimental results of oxidative steam reforming of ethanol reforming over Ni-based catalysts is described by the reaction pathway reported in Eq.4-7. Methane oxidation (Eq. 5) is an instantaneous and irreversible reaction with no influence on the kinetic study (McIntosh and van den Bossche, 2011). Ethanol decomposition was described through a power-low reaction rate (Ciambelli et al., 2010) while the model proposed by Xu and Froment (1989) was assumed for Eq. 6-7. The expression for the reaction rates are reported in Table 2. k_{CO}, k_{H2}, k_{CH4} and k_{H2O} indicates the adsorption constants while K_{eqi} refers to the equilibrium constants of the reactions, calculated by means of the software Gaseq. The Euler method was used to solve the mass balance equations over the length of an isothermal catalytic bed; the kinetic parameters were optimized by the means of a least square analysis based on the minimization of the sum of the residual squares of the experimental and predicted molar fractions.

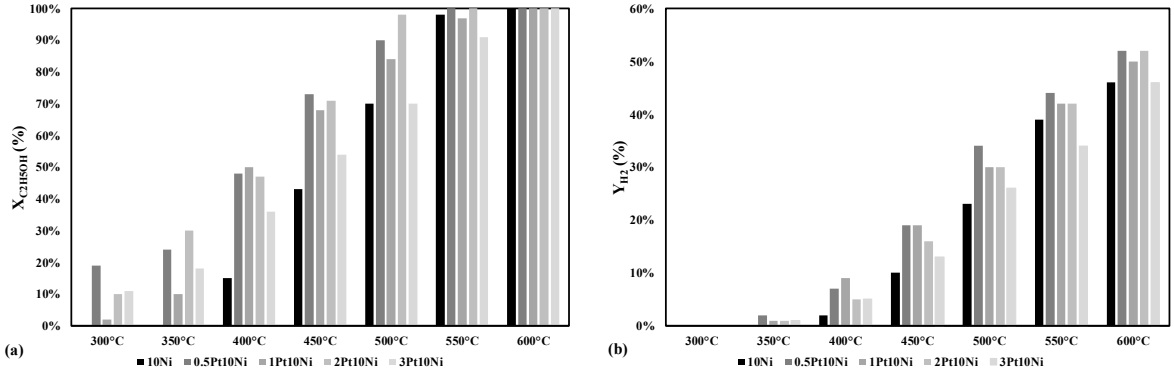

Figure 2: Ethanol conversion (a) and hydrogen yield (b) during OESR; H_2O/C_2H_5OH=4, O_2/C_2H_5OH=0.5, T=300-600°C, WHSV=62 h^{-1}.

$$C_2H_5OH \rightarrow H_2 + CH_4 + CO \quad \Delta H^{\circ}_{298K} = 49.9\ kJ/mol \quad \text{(r1)} \tag{4}$$

$$CH_4 + 2O_2 \rightarrow 2H_2O + CO_2 \quad \Delta H^{\circ}_{298K} = -802.6\ kJ/mol \quad \text{(r2)} \tag{5}$$

$$CH_4 + H_2O \leftrightarrow CO + 3H_2 \quad \Delta H^{\circ}_{298K} = 206\ kJ/mol \quad \text{(r3)} \tag{6}$$

$$CO + H_2O \leftrightarrow CO_2 + H_2 \quad \Delta H^{\circ}_{298K} = -41\ kJ/mol \quad \text{(r4)} \tag{7}$$

Figure 3 compares the experimental points and the curves predicted by the model for the 0.5Pt10Ni and 10Ni catalyst. The model assures a fairly good agreement with the experimental data, especially at high temperatures. Below 500°C, a reduced predictive capacity of the model is observed, which can be linked to the non-completion of carbon balances: due to the very low contact time selected, coke deposition occurred, thus reducing CO, CO_2 and CH_4 yields.

The kinetic investigation allowed evaluating the pre-exponential factors (k_o) and the activation energies (E_a) for r1, r3 and r4 over the two catalysts and the results are reported in Table 3. Pt addition had a positive impact on the performance of the monometallic sample, thus resulting in a sensible reduction of activation energy, especially for ethanol decomposition. This result suggests that platinum promotes the first step of the reaction pathways, thus favouring the formation of CH_4, CO and H_2. Methane steam reforming and water gas shift reactions are also faster in the presence of 0.5Pt10Ni/CeO_2-SiO_2 catalyst which, therefore, assured improved hydrogen yield compared to the monometallic formulation.

Table 2: Expression for the reaction kinetics.

Reaction	Expression
r1	$k_1 P_{C_2H_5OH}^{0.5}$
r3	$\dfrac{k_2 \cdot \left(P_{CH_4}.P_{H_2O} - \dfrac{P_{H_2}^3 \cdot P_{CO}}{K_{eq2}}\right)}{P_{H_2}^{2.5} \cdot \left(1 + K_{co} \cdot P_{co} + K_{H_2} \cdot P_{H_2} + K_{CH_4} \cdot P_{CH_4} + K_{H_2O} \cdot P_{H_2O}/P_{H_2}\right)^2}$
r4	$\dfrac{k_3 \cdot \left(P_{CO}.P_{H_2O} - \dfrac{P_{H_2} \cdot P_{CO}}{K_{eq3}}\right)}{P_{H_2} \cdot \left(1 + K_{co} \cdot P_{co} + K_{H_2} \cdot P_{H_2} + K_{CH_4} \cdot P_{CH_4} + K_{H_2O} \cdot P_{H_2O}/P_{H_2}\right)^2}$

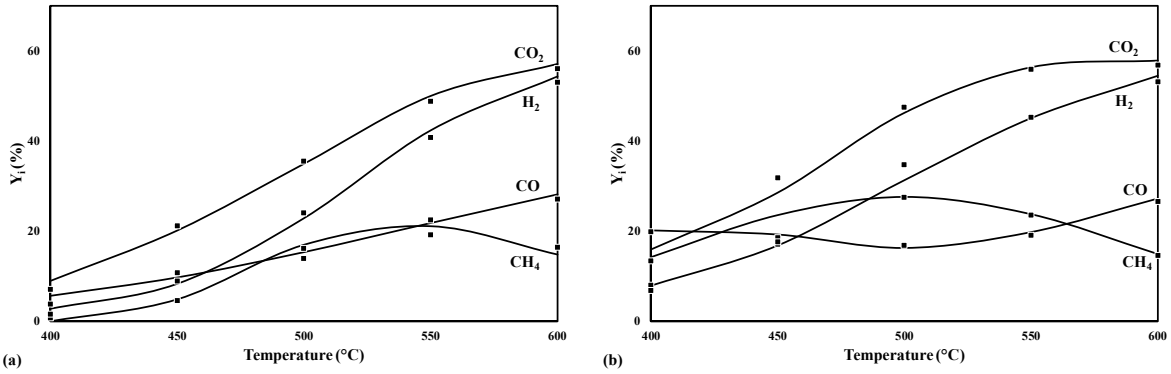

Figure 3: Model (continuous lines) and experimental (square) products yield for the (a) Ni and (b) 0.5Pt10Ni/CeO_2-SiO_2 catalyst.

Table 3: Pre-exponential factors (ko) and activation energies (Ea) for the reactions in Table 2 estimated for the activity results over 10Ni and 0.5Pt10Ni/CeO_2-SiO_2 catalysts.

Reaction	10Ni/CeO_2-SiO_2		0.5Pt10Ni/CeO_2-SiO_2	
	ko ($mol \cdot Pa^n \cdot s^{-1} \cdot g_{cat}^{-1}$)	Ea ($kJ \cdot mol^{-1}$)	ko ($mol \cdot Pa^n \cdot s^{-1} \cdot g_{cat}^{-1}$)	Ea ($kJ \cdot mol^{-1}$)
r1	$4.7 \cdot 10^{-1}$	76	$1.9 \cdot 10^{-3}$	38
r3	$3.7 \cdot 10^{3}$	70	$1.3 \cdot 10^{3}$	61
r4	$2.5 \cdot 10^{-5}$	30	$2.3 \cdot 10^{-5}$	26

4. Conclusions

In this work, oxidative steam reforming of ethanol has been investigated over Ni-based catalysts; the effect of Pt addition on catalyst activity was studied and a kinetic evaluation was also carried out to investigate the reaction mechanism over the monometallic and bimetallic catalysts. Pt addition had a beneficial effect on the performance of the Ni/CeO_2-SiO_2 sample. However, it was sufficient to employ platinum contents as low as 0.5 wt% to reach high hydrogen production rates, thus strongly reducing the catalyst price in comparison to previously employed formulations. The latter sample also reduces activation energies for ethanol decomposition, methane steam reforming and water gas shift reactions with respect to the Ni/CeO_2-SiO_2 sample: as a result, improved hydrogen yield between 300 and 600°C were measured.

References

Baruah R., Dixit M., Basarkar P., Parikh D., Bhargav A., 2015, Advances in ethanol autothermal reforming, Renewable and Sustainable Energy Reviews 51, 1345–1353.

Ciambelli P, Palma V, Ruggiero A., 2010, Low temperature catalytic steam reforming of ethanol. 2. Preliminary kinetic investigation of Pt/CeO2 catalysts, Applied Catalysis B: Environmental, 96, 190-197.

Du X., Zhang D., Shi L., Gao R., Zhang J., 2012, Morphology Dependence of Catalytic Properties of Ni/CeO2 Nanostructures for CO2 Reforming of Methane, The Journal of Physical Chemistry C, 116, 10009-10016.
Hernández M.A., J. González A. J., Suárez F., Ochoa C., Candela A.M., Cabeza I., 2018, Assessment of the Biohydrogen Production Potential of Different Organic Residues In Colombia: Cocoa Waste, Pig Manure and Coffee Mucilage, Chemical Engineering Transactions, 65, 247-252.
Liu S., Zhang K., Fang L., Li Y., 2008, Thermodynamic Analysis of Hydrogen Production from Oxidative Steam Reforming of Ethanol, Energy & Fuels, 22, 1365-1370.
McIntosh S, van den Bossche M., 2011, Influence of lattice oxygen stoichiometry on the mechanism of methane oxidation in SOFC anodes. Solid State Ionics, 192, 453-457.
Montero C., Valle B., Bilbao J., Gayubo A.G., 2014, Analysis of Ni/La2O3–αAl2O3 Catalyst Deactivation by Coke Deposition in the Ethanol Steam Reforming, Chemical Engineering Transactions, 37, 481-486.
Morales M., Segarra M., 2015, Steam reforming and oxidative steam reforming of ethanol over La0.6Sr0.4CoO3−δ perovskite as catalyst precursor for hydrogen production, Applied Catalysis A: General 502, 305–311.
Mulewa W., Tahir M., Amina N.A.S., 2017, Ethanol Steam Reforming for Renewable Hydrogen Production over La-Modified TiO2 Catalyst, Chemical Engineering Transactions, 56, 349-354.
Nishikawa J., Miyazawa T., Nakamura K., Asadullah M., Tomishige K., 2008, Promoting effect of Pt addition to Ni/CeO2/Al2O3 catalyst for steam gasification of biomass, Catalysis Communications, 9, 195-201.
Palma V, Ruocco C., Ricca A., 2015, Bimetallic Pt and Ni based foam catalysts for low-temperature ethanol steam reforming intensification, Chemical Engineering Transactions, 43, 559-564.
Palma V. Ruocco C., Meloni E., Ricca A., 2017, Coke-resistant Pt-Ni/CeO2-SiO2 Catalysts for Ethanol Reforming, Chemical Engineering Transactions, 57, 1675-1680.
Siang T.J., Vo D.V., 2017, Syngas Production from Combined Steam and Carbon Dioxide Reforming of Methane over Ce-modified Silicasupported Nickel Catalysts, Chemical Engineering Transactions, 56, 1129-1234.
Singh S., Nga N.T., Pham T.L., 2017, Metgas Production from Bi-reforming of Methane over La-modified Santa Barbara Amorphous-15 Supported Nickel Catalyst, Chemical Engineering Transactions, 56, 1573-1580.
Takeguchi T., Furukawa S., Inoue M., 2001, Hydrogen Spillover from NiO to the Large Surface Area CeO2-ZrO2 and Activity of the NiO/CeO2-ZrO2 for Partial Oxidation of Methane, Journal of Catalysis 202, 14-24.
Xu J, Froment G.F., 1989, Methane steam reforming, methanation and water-gas shift: I. Intrinsic kinetics. AIChE Journal, 35, 88-96.
Zhao S., Cai W., Li Y., Yu H., Zhang S., Cui L., 2018, Syngas production from ethanol dry reforming over Rh/CeO2 catalyst, Journal of Saudi Chemical Society, 22, 58-65.